J. Res. Inst. Catalysis, Hokkaido Univ., Vol. 29, No. 3, pp. 113 to 132 (1981)

MECHANISM OF HYDROGEN EVOLUTION REACTION ON GOLD IN AQUEOUS SULFURIC ACID AND SODIUM HYDROXIDE*)

By

Takeshi SASAKI**) and Akiya MATSUDA***)

(Received November 25, 1981)

Abstract

The hydrogen overvoltage on gold has been splitted into the components η_1 and η_2 which are caused respectively by the change of the free charge and the intermediate species on the electrode surface by the galvanostatic transient method in aqueous sulfuric acid and sodium hydroxide. It has been found that η_1 is responsible for the promotion of the rate of the electron transfer step which is the discharge of hydronium ion in acid and that of Na^+ ion in alkaline solutions, and that the recombination of adsorbed hydrogen atoms is rate-determining at low current densities in acid. In alkaline solutions, however, there appears an overvoltage component due to the specific adsorption of some species other than the intermediate Na atom which may result in the irregular variation of the polarization curves of the overall reaction.

Introduction

The mechanism of the hydrogen evolution reaction (h. e. r.) on gold has been discussed in acid solutions mainly based on the b-value of the Tafel slope of the polarization curves in steady conditions.[1~13] The Tafel slope in acid soultions, however, are noted for their wide variations among different authors. In alkaline solutions very few investigations have been reported[18] because of difficulties in obtaining reproducible results.

On the other hand, as pointed out by Horiuti *et al*,[14] the theoretically predicted b-value may vary from 30 mV to the values higher than 120 mV depending upon the mutual interaction among the intermediate species and activated complex of the reaction, even if the reaction proceeds through a single mechanism. Therefore the b-value of the Tafel slope cannot necessarily serve as a diagnostic criterion for the mechanism of the h .e. r.

*) This article is a part of Doctor thesis of T. S. in Hokkaido University (1974).

Present address: **) Faculty of Engineering, ***) Research Institute for Catalysis, Hokkaido University, Sapporo, 060 Japan.

It is desirable to divide experimentally the overall reaction into its constituent elementary steps and to compare directly their rates for the elucidation of the h. e. r. The present work is concerned with the determination of the rate and overvoltage of the constituent elementary steps of the h .e. r. on gold in acid and alkaline solutions by the galvanostatic transient method.[15]

Theoretical basis of the galvanostatic transient method

The hydrogen overvoltage η may be caused by the change of free charge density and adsorbed quantity of intermediate species on the electrode surface. These two components of overvoltage may be separately determined by a galvanostatic transient method by observing the transient of the electrode potential, $\eta-t$ curve, which is caused by adding a current pulse of constant height to the polarizing current.[15] If we observe the overvoltage transient at different time windows, then at the initial stage the change of η may be caused by the change of free charge on the electrode surface, since charging up of the electric double layer at the metal/solution interface may be much faster than the formation of adsorbed intermediate species on the electrode surface. Therefore we can obtain informations on the differential capacity C_D of the double layer and the time constant τ_1 of the electron leakage through the double layer from the analysis of the initial $\eta-t$ curve by the equation[15]

$$\ln\left(-\frac{\Delta i}{\dot{\eta}}\right)=\frac{t}{\tau_1}+C_D\,, \tag{1}$$

where Δi is the height of the current pulse and η signifies the time derivative of η, which can be identified with that of the electrostatic potential Ψ^* of the electrode surface in contact with the solution when Ψ^* is changed by charging up of the double layer.

As pointed out by Frumkin[16], Ψ^* can be expressed by the sum of several components

$$\Psi^*=\Psi_c^*+\chi_a+\chi_{S(M)}+\chi_S+\Psi_S\,, \tag{2}$$

where Ψ_c^* is the component of the electrostatic potential caused by the free charge on the electrode surface, χ_a is the surface potential due to the adsorbed

*) The electrochemical potential of the electron $\bar{\mu}_e$ in the electrode metal can be expressed as $\bar{\mu}_e=-\mathbf{F}(\Psi^*+W^*)=-\mathbf{F}(\Psi+W)$ in terms of the work function W^* of the electrode surface in contact with the solution or in terms of Ψ and W of the electrode surface in contact with the gas phase.

intermediate, $\chi_{S(M)}$ is the surface potential due to the specific orientation of the solvent dipole on the electrode surface, χ_S and Ψ_S are respectively the surface and Volta potentials of the soultion. In the present treatment the last three terms of Eq. (2) are assumed to be constant. Therefore it follows from Eq. (2) that

$$\frac{d\Psi^*}{dt} = \frac{d\Psi_i^*}{dt} + \frac{d\chi_a}{dt} , \tag{3}$$

and $\dot{\eta}$ in Eq. (1) can be identified with $\dot{\Psi}_i^*$. The overvoltage component η_1 caused by free charge on the electrode surface is given by the difference

$$\eta_1 = \Psi_i^* - \Psi_i^* (\mathrm{rev}) , \tag{4}$$

where $\Psi_i^* (\mathrm{rev})$ is Ψ_i^* at the reversible state of the h. e. r.

We assume here that the electron leakage through the double layer occurs only through the electron transfer step of the h. e. r. Then the time constant τ_1 in Eq. (1) is given by

$$\tau_1 = C_D r_1 \tag{5}$$

where r_1 is the reaction resistance of the electron transfer step which may be defined as

$$r_1 = -\left(\frac{\partial\Psi^*}{\partial i}\right)_{\chi_a} \tag{6}$$

and can be equalized to $-\dfrac{d\Psi_i^*}{di}$ by Eq. (3).

If we know the value of r_1 under a steady condition of polarization as a function of the current density i, then it may be possible to estimate the value of η_1 at current density i by the integration of Eq. (6)

$$\eta_1 = -\int_0^i r_1 di . \tag{7}$$

The overvoltage component η_2 caused by the adsorption of the reaction intermediate on the electrode surface may be given by

$$\eta_2 = \chi_a - \chi_a (\mathrm{rev}) = \eta - \eta_1 \tag{8}$$

under the presumption that $\chi_{S(M)} = \mathrm{const}$ at any electrode potential.

In this way it may be possible to elucidate the mechanism of the h. e. r. from the comparison of η_1 and η_2 in a steady state determined by the galvanostatic transient method*).

*) Recently Enyo[17] has discussed the role of the surface potential due to the intermediate species in the kinetic law of the h. e. r. His treatment will be discussed separately elsewhere.

Experimental method

The electric circuit for the observation of galvanostatic transients is shown in Fig. 1. The polarizing current i was supplied to the test (**T**) and the counter electrode (**C**) from storage battery (E) through high resistance ($\mathbf{R}_2$). The hydrogen overvoltage was determined by the potential difference between (**T**) and the reference electrode (**R**) observed on a memoscope oscilloscope screen (Hughs Arcraft Co., Model 105 A), the ohmic part due to the solution resistance being corrected on the oscilloscope screen (**M**) by a differential pre-amplifer. A current pulse Δi was superimposed on the polarizing current by a pulse generator (YHP Co. Model 214A) and the transient curves of overvoltage were recorded on the oscilloscope screen. A subsidiary circuit (**K**) was used for the compensation of the steady state overvoltage in order to observe only a transient part of overvoltage on the screen.

The arrangement of reaction apparatus is shown in Fig. 2, where (**A**) and (**B**) are vessels respectively for preparation and pre-electrolysis of solution

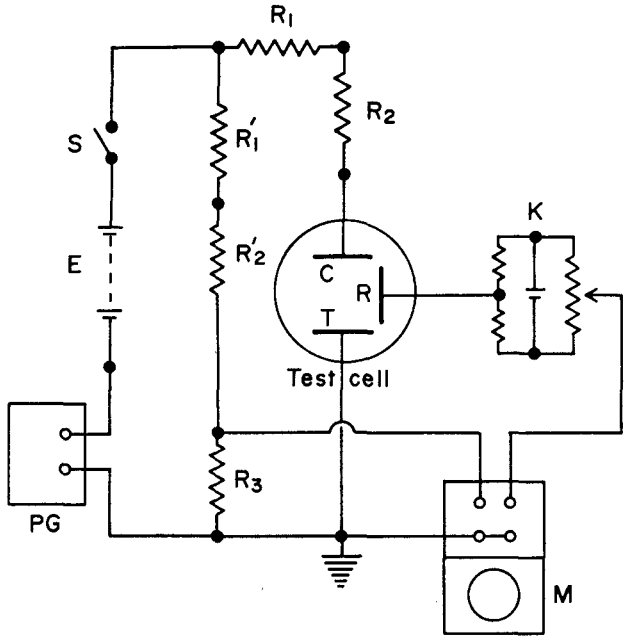

Fig. 1. Electric circuit for galvanostatic transient measurement. R_1, R_2, R_3: Resistances for current control and measurement and for compensation of ohmic part of overvoltage; K: compensation circuit for stationary overvoltage; PG, M: pulse generator and memoscope oscilloscope.

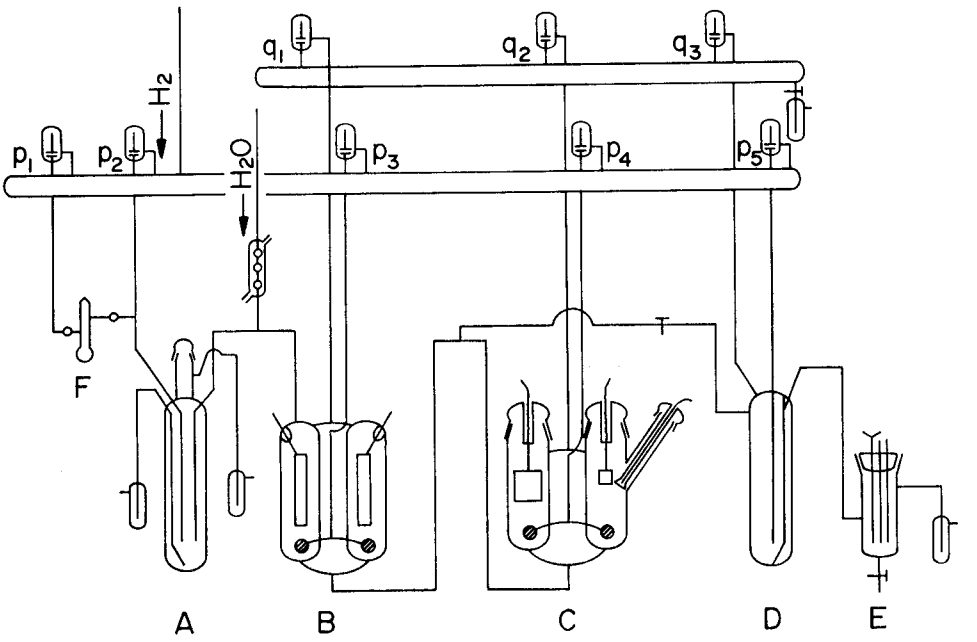

Fig. 2. Experimental apparatus. Vessels for preparation of solution (A), pre-electrolysis (B), test cell (C), solution storage (D), pH-measurement (E) and purified SO_3 gas (F). (p_1)–(p_5), (q_1)–(q_3) greaseless valves.

and (**C**) the test cell, all of which were made of quartz glass, and (**D**) for solution storage and (**E**) for pH measurement. All glass materials were preliminarily cleaned by steaming in hydrogen stream after treatments with hot mixture of concentrated nitric and sulfuric acids. Sulfuric acid solution was prepared from SO_3 gas distilled in vacuum and triplly distilled water. Alkaline solutions were prepared from sodium hydroxide and sodium sulfate recrystallyzed from analytical reagent. The solution in (**A**) was transferred to (**B**) by hydrogen pressure through greaseless stop cocks (p) and (q). After pre-electrolysis of the solution in (**B**) for about 50 hours with 20 mA, the solution was transferred into (**C**) by hydrogen pressure. After each run of kinetic measurements in (**C**) the solution was transferred into (**D**) which was used for the determination of pH in (**E**) or for the determination of the concentration by the titration method.

Gold foils of purity 99.99% (Johnson Matthey Co.) used for test and reference electrodes were purified by successive treatments with hot mixture of acids, hot distilled water, steaming in hydrogen stream and degassing under vacuum. Gold films prepared under vacuum by evaporating on to a ground glass surface were also used as the reference or test electrode.

Experimental results and discussion

(1) *Hydrogen evolution reaction in aqueous sulfuric acids*

The effect of anodic pre-treatment on the activity

The activity of the gold hydrogen electrode in sulfuric acid was found to increases by anodic treatment and its activity was maintained for about an hour and then decreases gradually with time.

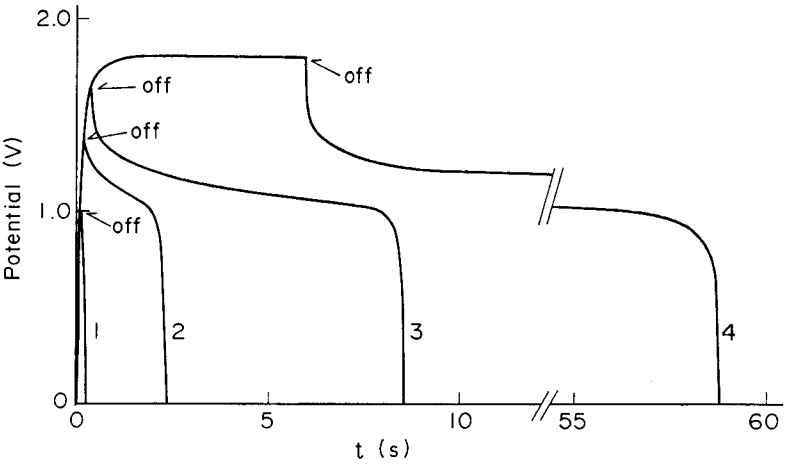

Fig. 3. Decay curves of electrode potential in 0.67 N H_2SO_4 after anodic treatment at 1.2×10^{-3} A/cm^2. Starting potential (vs. r. h. e.): curve (1)–1.0 V; curve (2)–1.4 V; curve (3)–1.64 V; curve (4)–1.8 V.

In order to get information on the surface state of the gold electrode after anodic treatments the potential decay in the anodic region was observed. A typical example of the decay curves in 0.67 **N** H_2SO_4 is shown in Fig. 3. The oxygen evolution was observed steadily at the potential 1.8 **V** and the current density 1.2×10^{-3} **A**/cm^2. It is seen from Fig. 3 that an arrest appears in the decay curve at 1.0–1.2 **V** which may be attributed to an oxidized state of the gold surface. The hydrogen adsorption can not practically be detected as seen from curve (1).

In order to find the change of the surface area by anodic treatments, the differential capacity C_D of the electrode was determined by the galvanostatic transient method. Fig. 4 shows the relation between log $(-\Delta i/\dot{\eta})$ vs. t obtained from the $\eta-t$ curves around the equilibrium potential after anodic pretreatments. The value of C_D was obtained from the extrapolation of the linear part in this figure on the basis of eq. (1). The values of C_D

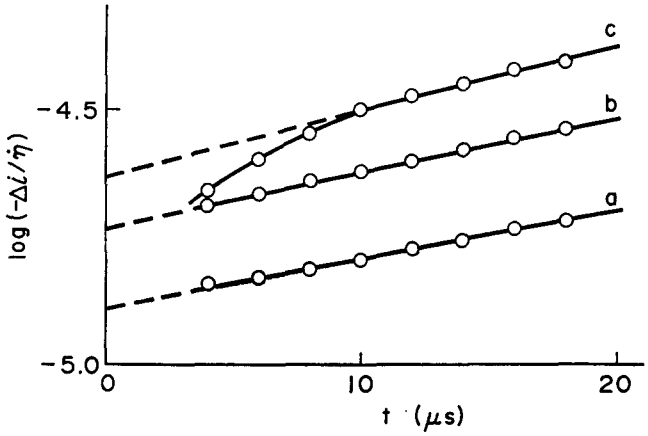

Fig. 4. Effect of anodic treatment of gold foil of geometrical area 0.6 cm^2 on the overvoltage transients at reversible potential in 0.3 N H_2SO_4, expressed by $\log(-\Delta i/\dot{\eta})$ vs. t relations. Line (a)-before anodic treatment; line (b)-after anodic treatment for 0.1 sec. at 1.2 V (vs. r. h. e.); line (c)-after anodic treatment for 10 sec. at 1.7 V (vs. r. h. e.).

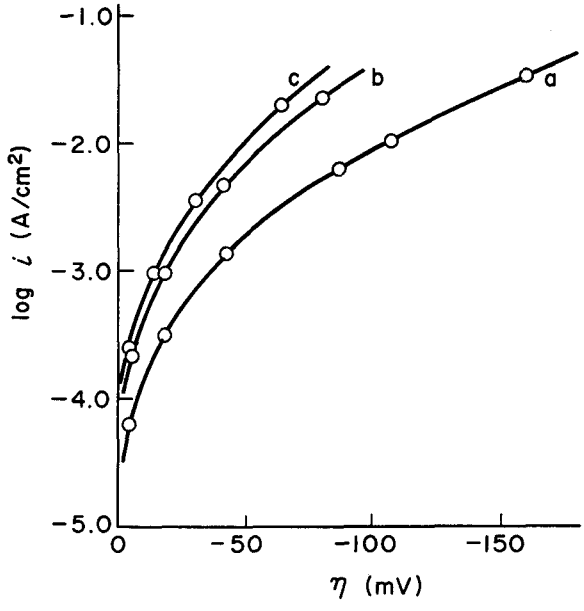

Fig. 5. Effect of anodic treatment on the steady state polarization curves obtained at the same condition of the electrode as in Fig. 4. Current density is expressed in terms of the true surface area estimated from the values C_D.

of the gold foil of geometrical area 0.6 cm^2 are respectively 13, 19 and 23 μF for curves (a), (b) and (c) respectively. It is seen from this figure that τ_1 remains practically unchanged, but C_D is increased by anodic treatments. The surface area of the gold electrode of geometrical area 0.6 cm^2 is estimated to be 0.72, 1.06 and 1.28 cm^2 from these C_D-values using 18 $\mu F/cm^2$ for the mercury electrode.[19] The increase of the surface area by anodic treatment may be attributed to the roughening of the electrode surface as suggested from the appearance of bending at the initial part of curve (c) in Fig. 4, as pointed out by Kunimatsu.[18] The steady state polarization curves which correspond to curves (a), (b) and (c) in Fig. 4 are shown in Fig. 5 expressed in terms of the current density using these surface areas. It is seen from Fig. 5 that the increase of activity of the gold electrode by anodic treatments cannot be explained by the increase of surface area of the electrode, contrary to the arguments of Kuhn and Byrne.[5] On the other hand τ_1 is practically not affected by anodic treatments, as seen from Fig. 4. It can be concluded from these facts that the increase in activity of the gold hydrogen electrode by anodic treatment may be attributed to the acceleration of elementary steps which follows the electron transfer step.

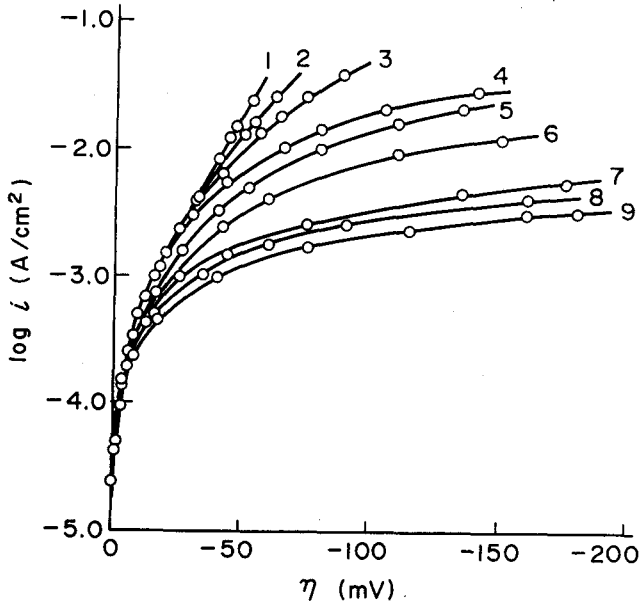

Fig. 6. Steady state polarization curves in aqueous H_2SO_4. Concentration (N): (1)-1.3, (2)-0.67, (3)-0.30, (4)-0.12, (5)-0.077, (6)-0.037, (7)-0.012, (8)-0.0053, (9)-0.0032.

The polarization curves for steady conditions

Fig. 6 shows the polarization curves in various concentration of H_2SO_4 obtained with an electrode of the highest activity after anodic treatment. These curves were observed at 25°C under strong stirring by forced hydrogen bubbles through sintered quartz glass.

As seen from Fig. 6, the log i vs. η curves coincide with each other at low current densities, whereas a strong concentration dependence appears

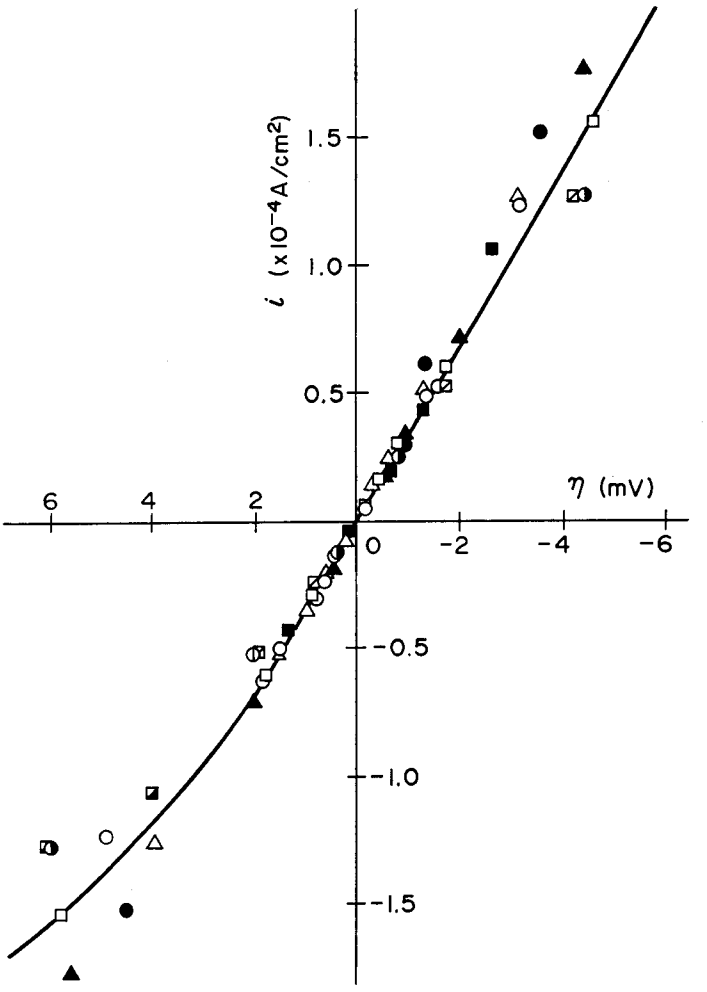

Fig. 7. i vs. η relation in steady states in the neighbourhood of the r. h. e. in aqueous H_2SO_4. The concentrations of solutions are the same as in Fig. 6.

at high current densities. Curve (1) which has Tafel slope of 28 mv is not affected by hydrogen bubbling, while curves (2)-(9) are strongly affected by stirring. The strong effect of hydrogen bubbling on the polarization curves may be explained by the diffusion of hydronium ion from the bulk of solution to the electrode surface. The Tafel slope of 28 mv in concentrated solutions may be explained either by the diffusion of molecular hydrogen from the electrode surface to the bulk of solution[20] or by the recombination of atomic hydrogen at low coverage[14,15] as rate-determining. As reported by Schuldiner and Hoare,[1] however, the polarization curves of Pd-hydrogen electrode show higher current density by about one order of magnitude than curve (1) in Fig. 6. It may be concluded from these facts that the hydrogen evolution on the gold electrode in sulfuric acid at low overvoltages is in favor of the recombination mechanism. Furthermore the $i-\eta$ curves in steady states in the neighbourhood of the reversible potential in various concentrations of H_2SO_4 from 1.3 to 3.2 10^{-3} N can well be expressed by a linear relation independent of the concentration of the solution as shown in Fig. 7. We obtain the exchange current density i_{ro} of the rate-determining step divided by its stoichiometric number ν_r as 4.3 10^{-4} A/cm^2 by the equation $i_{ro}/\nu_r=\frac{RT}{2\mathrm{F}}\Big/\left(\frac{d\eta}{di}\right)_{\eta=0}$ using the value of $\left(\frac{d\eta}{di}\right)_{\eta}=0$ calculated from Fig. 7.

Overvoltage components and kinetic law of electron transfer step

Fig. 8 (1) shows a series of $\log(-\Delta i/\dot{\eta})$ vs. t curves in 0.67 N H_2SO_4 obtained from the $\eta-t$ curves observed in various strady state conditions. As seen from this figure, C_D remains constant independent of the starting value of η ranging from 0 to -60 mV, whereas τ_1 decreases with increasing overvoltage ranging from 14 μs at $\eta=0$ to 7.8 μs at $-\eta=60$ mV. The values of r_1 calculated from τ_1 and C_D in Fig. 8 (1) are plotted against the steady current density i in Fig. 8 (2). The overvoltage component η_1 due to charging up of the electric double layer at the metal/solution interface can be calculated on the basis of eq. (7) by the graphical integration of the r_1-i curve in Fig. 8 (2). The $\log i$ vs. η_1 plot obtained from Fig. 8 (2) is shown in Fig. 9 by open circles in the solid line, which shows the theoretical relation[21]

$$i=i_{10}\left(e^{-\frac{F\eta_1}{2RT}}-e^{\frac{F\eta_1}{2RT}}\right), \tag{9}$$

where i_{10} is the exchange current density of the electron transfer step calculated by the equation using the reaction resistance r_{10} at $\eta=0$,

$$i_{10}=\frac{RT}{\mathrm{F}}\frac{1}{r_{10}} \tag{10}$$

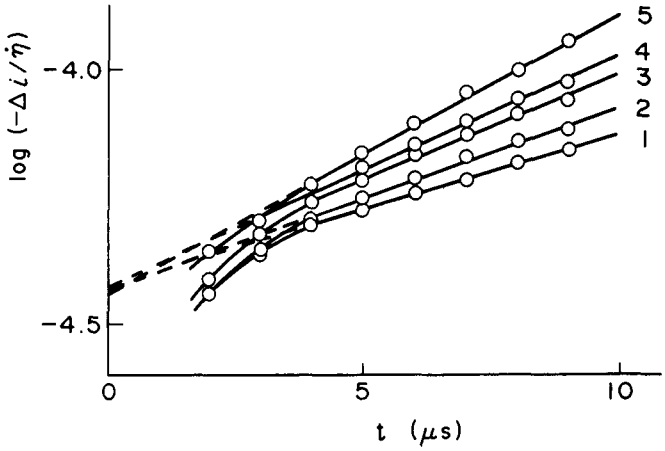

Fig. 8, (1). $\log(-\Delta i/\Delta\eta)$ vs. t relation in 0.67 N H_2SO_4 obtained from the transient curves at various steady conditions. Starting overvoltage $-\eta$ (mV): (1)-0, (2)-9, (3)-19, (4)-48, (5)-60.

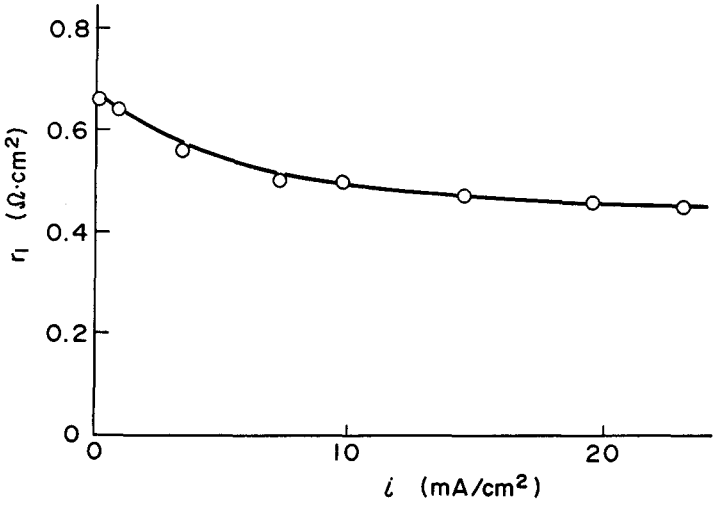

(2). i-dependence of the reaction resistance r_1 estimated from Fig. 9.

The $\log i$ vs. η_1 plot in 1.3 N and 0.3 N H_2SO_4 is also found on the theoretical line given by eq. (9) as shown in Figs. 9(2) and 9(3). It is surprising that the rate of the electron transfer step can be expressed in terms of the overvoltage compoent η_1 by a simple equation (9) as in the case of the Hg-hydrogen electrode in acid solution, although the range of η_1 in the present case is narrow. For comparison the polarization curve of the overall reaction is also shown in Figs. 9 by broken lines.

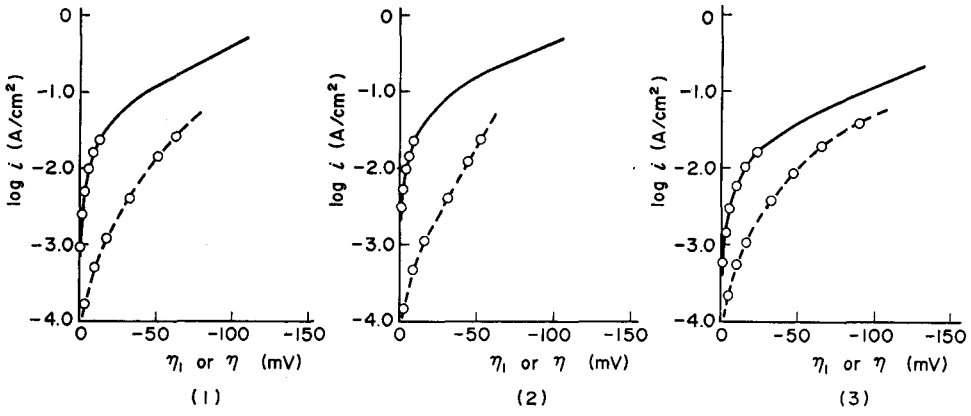

Fig. 9. Polarization curves in steady states for the electron transfer step (solid line) and overall reaction (broken line) in 0.67 N H_2SO_4 (1), in 1.3 N H_2SO_4 (2), in 0.30 N H_2SO_4 (3).

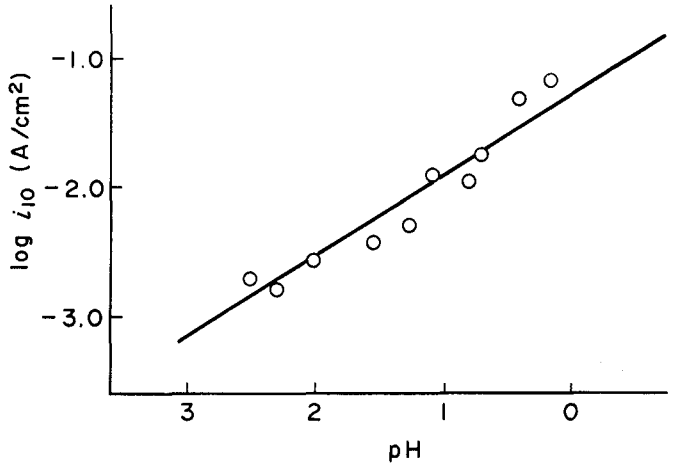

Fig. 10. pH-dependence of the exchange current density i_{10} of the electron transfer step in aqueous H_2SO_4.[24]

The pH-dependence of the exchange rate i_{10} of the electron transfer step[24] is shown in Fig. 10. The gradient of $\log i_{10}$ vs. pH equals about -0.6. It may be concluded from this result that the electron transfer step of the hydrogen evolution reaction on gold in sulfuric acid is the discharge of hydronium ion.

The overvoltage component η_2 due to the adsorbed intermediate species can be estimated as the difference $\eta-\eta_1$, from Fig. 9. Fig. 11. shows the relations between $\log i$ vs. η_2 in 1.3, 0.67 and 0.3 N H_2SO_4. As seen from

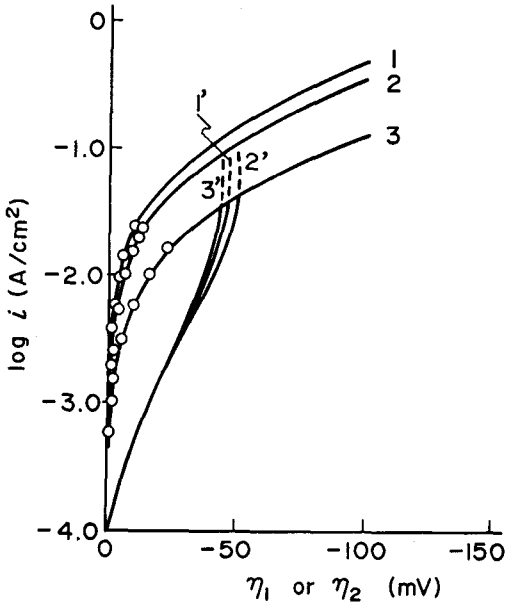

Fig. 11. Steady states polarization curves of the elementary steps of the hydrogen evolution reaction on gold in 0.3, 0.67 and 1.3 N H_2SO_4; 1, 2, 3-the discharge of hydronium ion; 1′, 2′, 3′-the recombination of adsorbed hydrogen atoms.

Fig. 11, $\log i$ vs. η_2 curves practically coincide with each other irrespective of pH of the solution with gradient about 29 mV. These polarization curves can be explained by the recombination of adsorbed hydrogen atoms at low surface coverage as predicted by Horiuti[14].

From the comparison of the $\log i$ vs. η_1 and $\log i$ vs. η_2 curves it can be seen that at low current densities the recombination of adsorbed hydrogen atoms is rate-determining. In fact the ratio of the exchange current densities i_{10}/i_{20} falls in the range 10–10^3 depending on the concentration of sulfuric acid, in conformity with $i_{10}/i_{20} \approx 10$ obtained by Matsushima and Enyo[22] by the isotopic tracer method, where i_{20} is the exchange current density of the recombination of adsorbed hydrogen atoms.

However, we cannot neglect the possibility that the discharge of hydronium ion in turn controls the rate at high current densities when the diffusion control of hydronium ion is eliminated.

(2) *Hydrogen evolution reaction in aqueous sodium hydroxide*
Polarization curves of the overall reaction

The behavior of the polarization of the gold hydrogen electrode in sodium

hydroxide is quite different from that in sulfuric acid. The activity of the electrode in alkaline solutions changes spontaneously with time, but it increases after anodic treatments at 1.7 V or higher potentials. However, the activity is not reproducible after anodic treatment. Such circumstances make it difficult to elucidate the mechanism of the hydrogen evolution reaction on the basis of the steady state polarization in alkaline solutions.

The effect of anodic pre-treatments on the steady state polarization in 8×10^{-3} and 0.56 N NaOH and in 0.43 N Na_2SO_4+0.01 N NaOH is shown in Figs. 12. It can be seen from these figures that the activity of the gold hydrogen electrode in alkaline solutions is lower than that in acid solutions by about 3~4 in order of magnitude. The distinctive feature of the polarization curves in alkaline solutions is that there appears a bending in the region lower than about $-\eta=250$ mV where the Tafel slope is much higher than 120 mV. In the region higher than 250 mV the polarization curves show usual behavior with the Tafel slope 120 mV. The bending of the polarization curve is more conspicuous with increasing pH of solution.

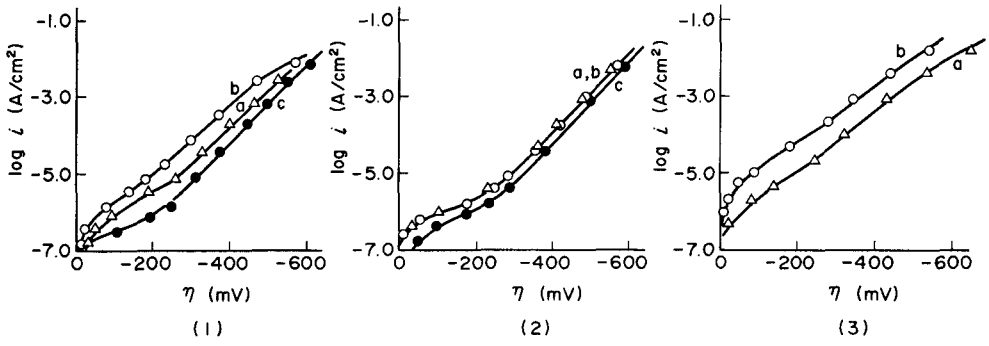

Fig. 12. Polarization curves of the overall reaction in steady state of the hydrogen evolution reaction on gold in alkaline solutions. (1)-0.008 N NaOH, (2)-0.56N NaOH, (3)-0.43 N Na_2SO_4+0.01 N NaOH. (a)-immediately after introduction of solution into cell; (b)-after anodic treatment for several sec. at 1.65 V (vs. r. h. e.); (c)-after several hours from anodic treatment.

In order to clarify the bending of the polarization curve, the pseudo-capacity of the electrode was determined from the decay curves of overvoltage by the following equation[23]

$$C_p=-\frac{i}{\dot{\eta}}. \tag{11}$$

The η-dependence of C_p in various solutions is shown in Fig. 13. As seen

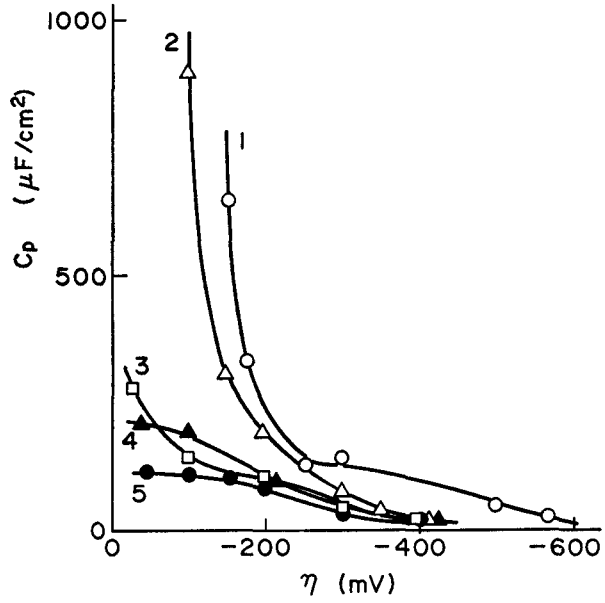

Fig. 13. η-dependence of the pseudo-capacity of the gold hydrogen electrode in alkaline solutions: (○) 0.56 N NaOH, (△) 0.022 N NaOH, (□) 0.008 N NaOH, (●) 0.43 N Na_2SO_4 (pH=12.1), (▲) 0.065 N Na_2SO_4 (pH=10.8).

from this figure, the high differential capacity is obtained in the overvoltage region where the bending of the polarization curve appears and the value of C_p is much higher in sodium hydroxide than in sodium sulfate solution. In high overvoltage region of the Tafel slope 120 mV, C_p practically equals C_D. The bending of the polarization curve may therefore be explained by the shift of the Volta potential of the electrode toward negative side due to a variety of specific adsorption depending on the composition of the solution. The reason of the shift of the Volta potential which may result in the bending of the polarization curve will be discussed later after the specification of the reaction intermediate.

Kinetic law of the electron transfer step

Fig. 14 shows a series of $\log(-\Delta i/\dot{\eta})$ vs. time curves in 4.3×10^{-2} N NaOH obtained from the $\eta-t$ curves started from various steady conditions. As seen from the figure, C_D remains constant independent of η in the range from 0 to -720 mV. The increase of C_D by anodic treatment was not observed in alkaline solutions. The value of τ_1 remains constant at 460 μsec in the range of $-\eta$ from 0 to 400 mV, while in the range $-\eta>400$ mV it decreases with increasing overvoltage, for example $\tau_1=89$ μsec at $-\eta=$

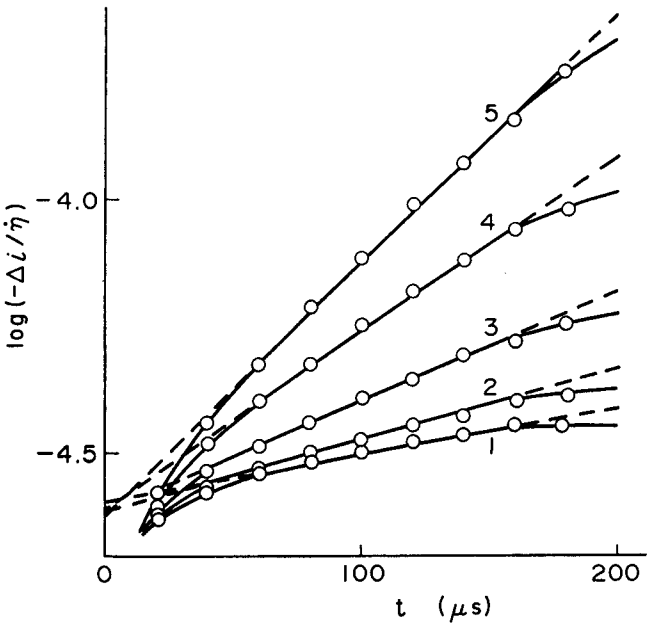

Fig. 14, (1). $\log(-\Delta i/\dot{\eta})$ vs. t relation obtained from the overvoltage transients at different stationary conditions in 0.043 N NaOH. Starting overvoltage $-\eta$ (mV): (1) 0~400, (2) 590, (3) 610, (4) 660, (5) 720.

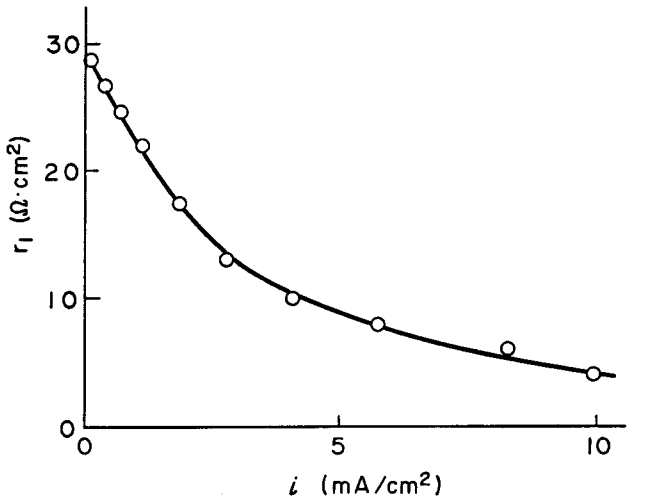

(2). i-dependence of the reaction resistance r_1 estimated from Fig. 14, (1).

716 mV. The values of r_1 calculated from Fig. 14 (1) are plotted against the steady current density i in Fig. 14 (2). The value of η_1 can be obtained from the graphical integration of this curve. The $\log i$ vs. η_1 plot obtained is shown by open circles in solid line in Fig. 15 together with the polarization curve of the overall reaction. The solid line in these figures shows the theoretical line calculated by eq. (6) using the experimental value of i_{10}.

It can be seen from the comparison of $\log i$ vs. η_1 and $\log i$ vs. η curves that η_1 is quite small as compared with η in every solution used. As noted

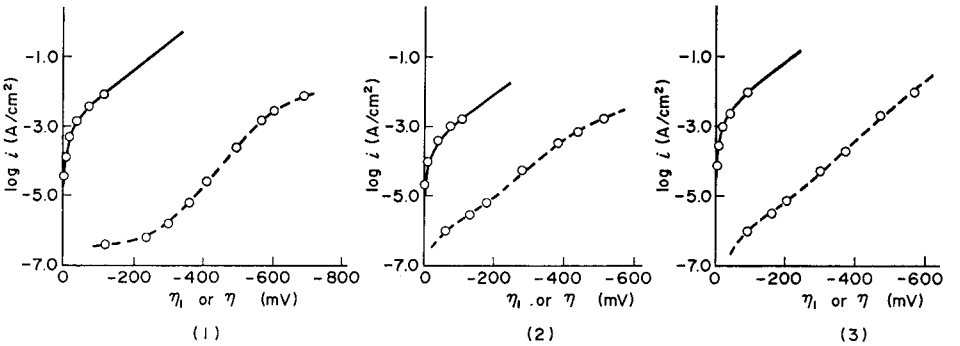

Fig. 15. Polarization curves in steady states for the electron transfer step (solid line) and overall reaction (broken line) in 0.043 N NaOH (1), in 0.007 N NaOH (2), in 0.43 N Na_2SO_4 (3).

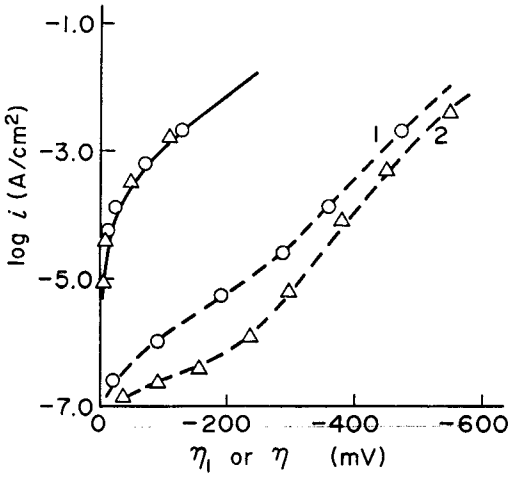

Fig. 16. Polarization curve of the electron transfer step in 0.008 N NaOH on gold of different activities of the overall reaction. Broken lines are polarization curves of the overall reaction: (1) active state, (2) inactive state.

in the previous section, the polarization curves of the overall reaction in alkaline solutions show wide variation depending on the pre-treatments of the electrode. However, the polarization curves $\log i$ vs. η_1 are not affected by pre-treatments of the electrode, as seen from Fig. 16, which shows the $\log i$ vs. η_1 curves obtained under the different activities of the overall reaction.

Fig. 17 shows the $\log i$ vs. η_1 curves in various concentration of sodium

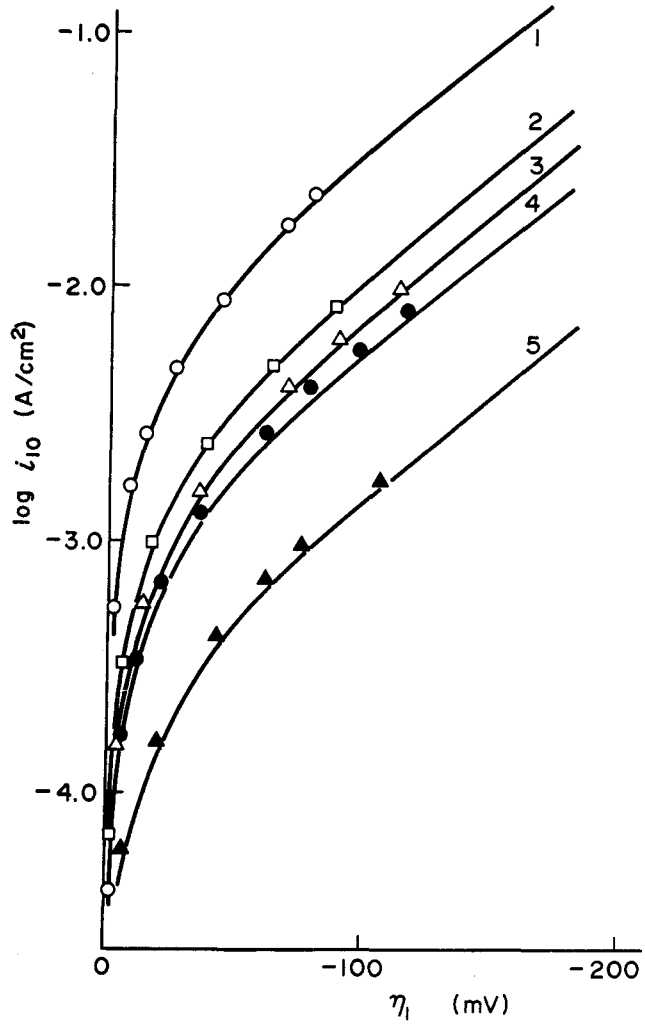

Fig. 17. Polarization curves of the electron transfer step of the h. e. r. in alkaline solutions; (1) 1.1 N NaOH, (2) 0.43 N Na_2SO_4 (pH = 12.1), (3) 0.043 N NaOH, (4) 0.022 N NaOH, (5) 0.007 N NaOH.

hydroxide or sodium sulfate.[25] The solid line in this figure shows the theoretical one given by Eq. (9). The log i vs. η_1 curve strongly depends on the concentration C_{Na^+} of Na^+ ion, as seen from this figure, and log i_{10} shows linear increase with increasing log C_{Na^+} with gradient 1/2, as shown in Fig. 18. It can be concluded from these facts that the electron transfer step of the h. e. r. on gold in sodium hydroxide is the discharge of Na^+ ion, but not the discharge of water molecule, and its rate can be expressed by Eq. (9) as a function of η_1.

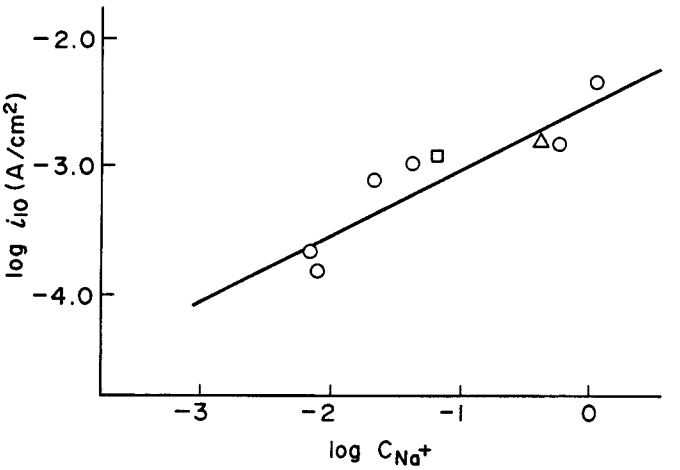

Fig. 18. Dependence of exchange current density of the electron transfer step on Na^+ ion concentration[25]; (○) NaOH solution; (△) 0.43 N Na_2SO_4 (pH 12.1); (□) 0.065 N Na_2SO_4 (pH 10.8).

On the other hand, the gold h. e. in alkaline solutions indicated the bending of the polarization curves of the overall reaction and has high values of the pseudo-capacity C_p in the overvoltage region corresponding to the bending of the polarization curves, as described in a previous section. The values of C_p in this region strongly depend on pH of the solution rather than the concentration of sodium ion, as seen from Fig. 12. Therefore the Volta potential change of the electrode may be caused in this region by the specific adsorption of some species in addition to the intermediate Na atom, probably OH^- ion. This may be one of the reasons why the h. e. r. on gold in alkaline solutions is irreproducible and has high overvoltage as compared with that in acid solution.

References

1) S. Schuldiner and J. P. Hoare, J. Phys. Chem., **61**, 705 (1957).
2) S. Schuldiner, J. Electrochem. Soc., **99**, 488 (1952).
3) K. Gossner and C. Loeffler, Z. physik. Chem., Frankfurt **37**, 115 (1963).
4) M. Breiter, H. Kammermaier and C. A. Knorr, Z. Elektrochem., **60**, 454 (1966).
5) A. T. Kuhn and M. Byrne, Electrochim. Acta, **16**, 391 (1971).
6) E. D. Levin and A. L. Rotinyan, Elektrokhimiya, **8**, 240 (1972).
7) M. Breiter and R. Clamroth, Z. Elektrochem., **58**, 493 (1954).
8) G. M. Sdhmid, Electrochim. Acta, **12**, 449 (1967).
9) J. O'M. Bockris and R. Parsons, Trans. Faraday Soc., **44**, 860 (1948).
10) D. J. G. Ives and S. Swaroopa, J. Chem. Soc., 3489 (1955).
11) A. Hickling and F. W. Salt, Trans. Faraday Soc., **36**, 1226 (1940).
12) B. E. Conway, Proc. Roy. Soc., **A 256**, 128 (1960).
13) N. Pentland, J. O'M. Bockris and E. Sheldon, J. Electrochem. Soc., **104**, 182 (1957).
14) J. Horiuti, J. Res. Inst. Catalysis, Hokkaido Univ., **4**, 55 (1956).
15) A. Matsuda and J. Horiuti, J. Res. Inst. Catalysis, Hokkaido Univ., **6**, 231 (1958).
16) J. Res. Inst. Catalysis, Hokkaido Univ., A. Matsuda and R. Notoya, **14**, 165 (1966); **18**, 53 (1970); **18**, 59 (1970); R. Notoya and A. Matsuda, **14**, 192 (1966); **15**, 247 (1968); T. Ohmori and A. Matsuda, **15**, 201 (1968); **17**, 39 (1969); **21**, 70 (1973); A. Matsuda and T. Ohmori, **10**, 215 (1962); R. Notaya, **19**, 17 (1971). R. Notoya, Shokubai (Catalyst), **12**, 61 (1970). Denki Kagaku, A. Matsuda, **33**, 484 (1965); A. Matsuda and R. Notoya, **34**, 619 (1966); K. Tachibana and A. Matsuda, **41**, 332, 407 (1973).
17) A. Frumkin, *Potentsialy Nulevogo Zaryada*, Nauka, Moscow, 1979, p. 177.
18) M. Enyo, J. Res. Inst. Catalysis, Hokkaido Univ., **29**, 1 (1981).
19) K. Kunimatsu, J. Res. Inst. Catalysis, Hokkaido Univ., **20**, 1, 20 (1972), **21**, 77 (1972).
20) M. Vorsina and A. N. Frumkin, Acta Physicochim. U. S. S. R., **17**, 295 (1943).
21) L. Kandler, C. A. Knorr and C. Schwitzer, Z. Physik. Chem., **A 180**, 281 (1937).
22) A. N. Frumkin, V. S. Bagotzky, Z. A. Jofa and B. N. Kabanov, *Kinetics of Electrode Processes*, Moscow Univ. Press (1952), p. 172.
23) T. Matsushima and M. Enyo, Electrochim. Acta, **19**, 117 (1974).
24) R. Notoya and A. Matsuda, J. Res. Inst. Catalysis, Hokkaido Univ., **14**, 198 (1966).
25) T. Sasaki and A. Matsuda, Chem. Lett., 141 (1974).
26) T. Sasaki and A. Matsuda, J. Res. Inst. Catalysis, Hokkaido Univ., **21**, 157 (1973).